Magnetohydrodynamic Flow and Heat Transfer of an Upper-Convected Maxwell Fluid Due to a Stretching Sheet

R. C. Bataller[1]

Abstract: We present a numerical study of the flow and heat transfer of an incompressible upper-convected Maxwell (UCM) fluid in the presence of an uniform transverse magnetic field over a porous stretching sheet taking into account suction at the surface as well as viscous dissipation and thermal radiation effects. Selected similarity analyses have been carried out by means of a numerical implementation. The effects on the velocity and temperature fields over the sheet of the parameters like elasticity number, suction velocity, magnetic parameter, radiation parameter, Prandtl number and Eckert number are also analyzed.

Keywords: MHD flow; UCM fluid; Permeable stretching sheet; Viscous dissipation; Thermal radiation

1 Introduction

The continuous moving surface heat transfer problem is relevant since it has many engineering applications such as production of both metal and polymer sheets, thermal and moisture treatment of materials, production of crystalline materials and glass sheets, paper and textile industries, production of continuous stretched stripes or filaments by drawing them through a quiescent fluid and many others. The quality of the final product depends on the skin friction coefficient as well as the rate of heat transfer at the stretching surface. In order to obtain the desired characteristics of the final product, the involved fluid in these cases is treated as a non-Newtonian fluid. Certainly, water is widely utilized as the cooling medium, but the use of polymeric additives could present some advantages: Rajagopal et al. (1984). This class of flow was first studied by Sakiadis (1961) for moving and inextensible surfaces and later extended by Crane (1970) to the semi-infinite fluid flow driven by a linearly stretching surface.

---
[1] Departamento de Física Aplicada, Escuela Técnica Superior de Ingenieros de Caminos, Canales y, Puertos, Universidad Politécnica de Valencia, 46071 Valencia, Spain.

Recently, boundary layer flow for non-Newtonian fluids with or without heat transfer has been studied by Cortell (1994), (2006a), (2007d), for a second grade fluid, by Bhatnagar et al.(1995) for an Oldroyd-B fluid, by Sadeghy et al.(2005) for an upper-convected Maxwell (UCM) fluid in a Sakiadis flow configuration, by Abbas et al. (2006) for an UCM fluid flow in a porous channel, and also Cortell (2008b) has analyzed flow and heat transfer in the presence of thermal radiation by modelling viscoelastic properties with the help of the FENE-P (finitely extensible nonlinear elastic fluids) constitutive equation. In addition, very recently, Cortell (2010) has analyzed the magnetohydrodynamic (MHD) viscous flow influenced by a shrinking sheet with suction.

Flow kinematics can also be modified with the help of a sufficiently strong magnetic field applied to an electrically conducting fluid surrounding a stretching sheet: Cortell (2005a), (2006b). Specifically, in flows involving heat transfer, Bird et al. (1987), it has been shown that might be some advantages if the fluid surrounding the sheet can be made viscoelastic by using polymeric additives: Dandapat and Gupta (1989), Cortell (2007a). On the other hand, one can also resort to suction/blowing in order to modify flow kinematics, Cortell (2005b). Furthermore, MHD free convection flow of a non-Newtonian power-law fluid near a stretching sheet has been investigated by Abo-Eldahad and Salem (2004). MHD mixed convection owing to the stagnation flow against a heated vertical semi-infinite permeable surface is analyzed by Abdelkhalek (2006), and, the unsteady boundary-layer flow due to impulsive starting from rest of a stretching surface in a rotating fluid was studied by Nazar et al. (2004).

Usually, our proposed problems in the present area are solved by using boundary-layer theory along with the concept of similarity solution. The obtained ODE still presents a difficult problem to solve due to the lack of enough physical boundary conditions. Nowadays, we currently take into account for problems of Sakiadis/Crane type (i.e., $f' \to 0$ *as* $\eta \to \infty$), the conditions at infinity $f'' \to 0$ *as* $\eta \to \infty$(f being the non-dimensional stream function) for momentum transfer problems, and $\theta' \to 0$ *as* $\eta \to \infty$(θ being dimensionless temperature) for heat transfer problems, respectively. See, for example, Cortell (1994), (2006a, c), (2007b, c). It is worth mentioning here that the aforementioned conditions at infinity have been taken into consideration in our studies since early 1990s, Cortell (1994). Following the above cited procedure, Cortell (2005c), (2008a) studied numerically momentum transfer characteristics as far as Newtonian fluids are concerned, and in Liu (2008) the Lie-group shooting method is applied on the Blasius and Falkner-Skan equations. The stability and accuracy of the present procedure are strengthened by several very recent comparisons of earlier obtained results, Abel et al. (2009), Chen (2009) in related fluid dynamics problems.

The problem under investigation (i.e., MHD flow and heat transfer of an UCM fluid) is highly non-linear and these classes of problems are not easy to examine. Therefore, many applied mathematicians and numerical analysts have also recently paid much attention in developing suitable algorithms for solving these problems. The highly non-linear ordinary differential equation (ODE) appeared from the non-linear UCM fluid flow problem leads to the need of a numerical treatment. In fact, a systematic analysis of the stagnation-point flow of UCM fluids has been carried out by Sadeghy et.al. (2006), and furthermore, heat source and thermal radiation effects on MHD viscoelastic fluid flow past a stretching sheet were very recently studied by Singh (2008). Thermal radiation effects on heat transfer of boundary layer flow may also play an important role in controlling heat transfer in processes involving high temperatures such as polymer processing industry, nuclear power plants, thermal energy storage, gas turbines, solar power technology, Cortell (2008c).

In recent years, MHD flows of UCM fluids above stretching sheets have also been addressed by some researchers: Amir et al. (2009), Hayat et al. (2006), Aliakbar et al. (2009). The most recent attempt for the UCM flow with thermal radiation, but without suction at the plate has been developed by Aliakbar et al. (2009); however, Cortell (2006d) has already analyzed suction effects on MHD second grade fluid flow and heat transfer, and also Cortell (2007b) gave numerical results for momentum and mass transfer characteristics in two viscoelastic fluid flows (i.e., second-grade and second order non-Newtonian). Considerable novelty of this work is achieved due to the fact there have only been a small number of studies in that classes of flows where, probably first time, suction effects on temperature field have been assumed.

In order to obtain several realistic solutions where non-isothermal conditions at the flat sheet are present, in this paper we study UCM flow and heat transfer on a linearly stretching sheet in the presence of an uniform transverse magnetic field for two different types of thermal boundary conditions on the sheet with power-law surface temperature of second degree, that is, prescribed surface temperature (PST case) and prescribed heat flux at the plate (PHF case).The surface is held at a temperature $T_w(x)$ higher than the temperature T_∞ of the ambient fluid. Another effect which bears great importance on heat transfer is viscous dissipation. When the viscosity of the fluid and/or the velocity gradient is high, the dissipation term becomes important; although it disappears at infinity. Consequently, the effects of viscous dissipation are also included in the energy equation. For many cases, such as polymer processing, which is at very high temperature, Winter (1977), viscous dissipation plays an important role and it has been shown to be highly important.

Very recently, the homotopy analysis method (HAM) has been addressed to solve

flows of UCM fluids with or without magnetic field, Hayat and Sajid (2007), Alizadeh-Pahlavan and Sadeghy (2009), Hayat and Abbas (2008), and in our research, numerical and stable results are also obtained at large elasticity and/or magnetic number by using a 4th order Runge-Kutta method along with shooting method. The mechanical characteristics of the flow are also analyzed. Furthermore, it will be underlined that the role of the velocity gradient at infinity (i.e., $f''(\infty)$) is of key relevance for our results from which the entrainment velocity $f_\infty = f(\infty)$ can also be studied. We extend our own earlier researches for UCM flows, Bataller (2010), and analyze the effects on both momentum and heat transfer problems of six physical parameters: i) the elasticity number K of the Maxwellian fluid, ii) the magnetic parameter M, iii) the suction parameter R, iv) the Prandtl number σ, v) the Eckert number $E_c(E_c')$ and vi) the radiation parameter N_R, which will have a positive value throughout this research. In order to describe the above cited physical features easily and accurately, the numerical solution of a highly non-linear problem governed by an ordinary differential equation is, in our opinion, a suitable choice.

In Sect. 2 we shall consider the analysis of the UCM flow under suction and magnetic field effects; in Sect. 3 we shall examine the thermal problem when the viscous dissipation and thermal radiation are included and the influence on the numerical results of these additional effects will also be discussed. Finally, some conclusions end the paper in Sect. 4.

2   The flow

Let us suppose a steady, laminar and two-dimensional flow of an incompressible, electrically conducting and Boussinesq viscoelastic UCM fluid subject to a transverse uniform magnetic field B_0 which is applied in the positive y-direction past a flat, horizontal and porous sheet coinciding with the plane $y = 0$, the flow being confined to $y > 0$. The motion of the fluid is generated due to linear stretching of the sheet with the application of two equal and opposite forces, which are applied along the x-axis so that the wall is stretched keeping the origin fixed. The velocity of the fluid far away from the plate is equal to zero whereas fluid suction is imposed at the plate surface. The fluid has constant kinematic viscosity and thermal diffusivity. The magnetic Reynolds number is considered to be small so that the induced magnetic field is negligible in comparison to the applied magnetic field. The fluid is considered to be gray; absorbing-emitting radiation but non-scattering medium and the Rosseland approximation is used to describe the radiative heat flux. The system of continuity and momentum equations can be written, in the usual notation, as (see Sadeghy et al. (2006), Aliakbar et al. (2009)):

$$\frac{\partial u}{\partial x} + \frac{\partial v}{\partial y} = 0, \tag{1}$$

$$u\frac{\partial u}{\partial x} + v\frac{\partial u}{\partial y} = \upsilon\frac{\partial^2 u}{\partial y^2} - \beta\left[u^2\frac{\partial^2 u}{\partial x^2} + v^2\frac{\partial^2 u}{\partial y^2} + 2uv\frac{\partial^2 u}{\partial x\partial y}\right] - \frac{\sigma_0 B_0^2}{\rho}u, \tag{2}$$

We take x-axis along the surface, the y-axis being normal to it and u and v are the velocity components in x and y directions, respectively, υ is the kinematic viscosity, ρ is the density and β is the relaxation time of the fluid. Further, B_0 is the uniform magnetic field along the y-axis and σ_0 is the electric conductivity. The boundary conditions to the problem are

$$u = cx, \quad v = -v_w \ at \ y = 0, c > 0 \tag{3}$$

$$u \to 0 \ as \ y \to \infty. \tag{4}$$

In the second condition (3) $v = -v_w$ is the suction velocity.

The equation of continuity (i.e., Eq. (1)) is satisfied if we define the following new variables

$$u = cxf'(\eta), \ v = -(c.\upsilon)^{1/2}f(\eta) \tag{5}$$

where

$$\eta = \left(\frac{c}{\upsilon}\right)^{1/2} y, \tag{6}$$

and substituting into Eq. (2) gives

$$(f')^2 - ff'' + Mf' = f''' - K\left[f'''(f)^2 - 2ff'f''\right], \tag{7}$$

where $K = \beta c$ is the elasticity parameter, $f(\eta)$ denotes the dimensionless stream function and a prime determines differentiation with respect to η. Further, $M = \frac{\sigma_0 B_0^2}{\rho c}$ is the magnetic field parameter. The boundary conditions (3) and (4) becomes

$$f = R, \ f' = 1 \ at \ \eta = 0,$$

$$f' \to 0 \ as \ \eta \to \infty. \tag{8}$$

where $R = \frac{v_w}{(c\upsilon)^{1/2}}$ is the suction (>0) parameter.

We guess the missed $f''(0)$ value and integrate equations (7) along with boundary conditions (8) as an initial value problem by the fourth-order shooting Runge-Kutta method as explained in Cortell (2008b). The iterative procedure is stopped to give the velocity and velocity-gradient distributions when the boundary condition (8) at infinity is reached. Certainly other schemes are possible, and perhaps to be

preferred for specific kinds of problems, but ours has proved successful for all the numerical examples throughout the paper. Equivalent step sizes $\Delta\eta$ of 0.01 and 0.001 are used.

As far as flow kinematics is concerned, quantities of relevant physical interest are:

1. The entrainment velocity of the fluid f_∞ defined here as $f_\infty = f(\eta_\infty)$ with $f'(\eta_\infty) \approx 10^{-4}$. The corresponding η_∞ values are also given here in tabular form. Realize that from the second Eq.(5) we obtain $v_\infty = -(c.v)^{1/2} f_\infty$ and these quantities are related with the amount of fluid dragged by the sheet.

2. The thickness of the boundary layer δ defined as the value of the y coordinate for which $f'(\eta_\delta) = \frac{f'(0)}{100}$ holds. The corresponding η_δ values are also given here in tabular form.

A listing of the velocity gradient wall $f''(0)$ values at $R = 0.3$ (suction) and $M = 0.5$ is given in Table 1. The effect of increasing values of the elasticity number K is to decrease the magnitude of f_∞ largely in the boundary-layer. One can then see the strong effect of the elasticity level of the fluid on the flow kinematics. One further can detect that the values of $|f''(0)|$ increase with K. Hence the elasticity level of the Maxwell fluid increases the skin friction and this leads to a decrease in the boundary layer thickness as well as a diminution of the amount of fluid dragged by the sheet.

Table 1: The effect of the elasticity number K on flow characteristics for the case of suction ($R = 0.3$ and $M = 0.5$).

K	$-f''(0)$	η_δ	η_∞	f_∞
0	1.3838958	3.32	6.65	1.0225250
1	2.0863156	2.05	4.16	0.7547567
2	2.9498858	1.42	3.03	0.6181933
3	4.0212689	1.04	2.19	0.5338660
4	5.3857126	0.78	1.59	0.4757220
5	7.1874124	0.59	1.21	0.4327303
6	9.6842483	0.445	0.895	0.3993294
7	13.3850337	0.325	0.660	0.3724656
8	19.4525116	0.227	0.468	0.3502666
9	31.2523558	0.144	0.292	0.3315256
10	64.2650950	0.070	0.140	0.3154414

From the numerical calculations, it is observed that the sensitivity of η_δ, η_∞ and f_∞ with respect to the dimensionless velocity gradient $f''(0)$ at the wall is pro-

nounced and we also see that the parameter K affects the flow characteristics significantly. On the other hand, it can be found from Table 2 that $|f''(0)|$ increases with M for a given Maxwell fluid in the case of suction. However, one also sees that the effect of the parameter M is to decrease η_δ, η_∞ and f_∞. The effect of increasing values of the suction parameter R is to increase the magnitude of f_∞ largely in the boundary-layer, whereas parameter M decreases it. As far as the amount of fluid dragged by the sheet is concerned, one can conclude that, for fixed K, parameters M and R act in an opposite fashion. It is obvious from Table 2 that the entrainment velocity f_∞ increases with the increasing suction parameter R, while it decreases with the increasing magnetic field parameter M.

Table 2: The effect of the magnetic field parameter M and suction parameter R on flow characteristics of a Maxwellian fluid with $K = 0.3$.

K	R	M	$-f''(0)$	η_δ	η_∞	f_∞
0.3	0	1	1.4680536	3.03	6.65	0.664904
	0.3		1.7586223	2.55	5.46	0.858017
	0.6		2.1893104	2.06	4.16	1.050276
0.3	0.3	0.2	1.4586547	3.03	6.26	0.966269
		0.5	1.5789008	2.82	5.96	0.918409

In order to more fully characterize the behaviour of the numerical solutions with respect to the involving parameters, that is, K (elastic parameter), M (magnetic field parameter) and R (suction parameter) which govern this highly non-linear momentum transfer problem, representative dimensionless velocity and velocity gradient profiles at selected values of the elastic parameter K are shown in Fig.1. This Figure shows that, for $M = 0.5$ and $R = 0.3$ (suction), the effects of the fluid's elasticity are to decrease the dimensionless velocity $f'(\eta)$ at any given point above the sheet. In other words, the momentum boundary-layer thickness becomes thinner as the elastic parameter K increases.

Moreover, Fig. 2 depicts the changes in the $f'(\eta)$ and $f''(\eta)$ profiles at $R = 0.3$ with changes in K and M.

Furthermore, the influences of the magnetic parameter M on velocity profiles have also been investigated. In the case of suction (i.e., $R = 0.3$), Figure 2 demonstrates graphically that, for fixed K, the momentum boundary-layer becomes thinner as the magnetic field parameter M increases. This effect diminishes with increase in K. In other words, by an increase in the elasticity of the fluid, the effect of magnetic field on the velocity of fluid elements on the sheet appears to become less pronounced. It is further obvious that large elasticity and magnetic field numbers provide a lower influence of the magnetic parameter M onto velocity profiles. For a fixed value of
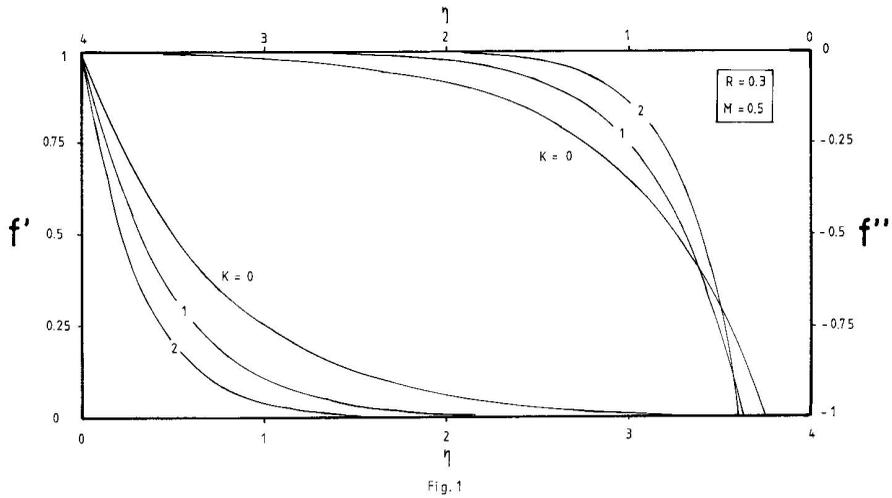
Figure 1: Velocity and velocity gradient profiles for selected values of *K* when *M* = 0.5 and *R* = 0.3 (suction).
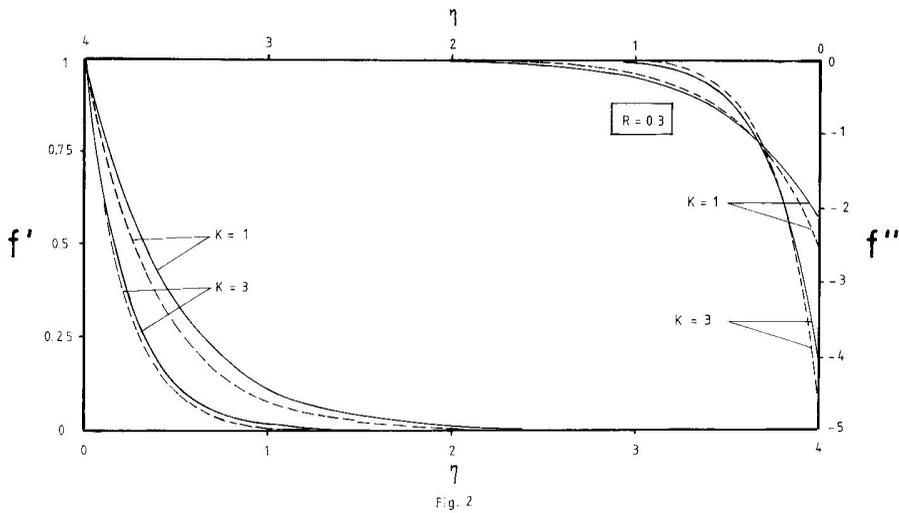
Figure 2: Velocity and velocity gradient profiles for selected values of *K* and *M* when *R* = 0.3 (suction). [*M* = 0.5 (solid line); *M* = 2 (broken line)].

R, the boundary layer thickness varies as K, which is characteristic of such flows. On the other hand, as was noted in the Introduction, one immediately sees from Figs. 1-2 how both f' and f'' tend simultaneously to zero at infinity as must be required from boundary-layer theory.

3 Heat transfer analyses

By using usual boundary layer approximations, the equation of the energy for temperature T in the presence of radiation and viscous dissipation is given by

$$u\frac{\partial T}{\partial x} + v\frac{\partial T}{\partial y} = \alpha\frac{\partial^2 T}{\partial y^2} + \frac{v}{c_P}\left(\frac{\partial u}{\partial y}\right)^2 - \frac{1}{\rho c_P}\frac{\partial q_r}{\partial y}, \tag{9}$$

where $\alpha = \frac{k}{\rho c_P}$ is the thermal diffusivity (k being the thermal conductivity), c_P is the specific heat of a fluid at constant pressure and q_r is the radiative heat flux.

Using the Rosseland approximation for radiation, Cortell (2008b), the radiative heat flux is simplified as

$$q_r = -\frac{4\sigma^*}{3k^*}\frac{\partial T^4}{\partial y}, \tag{10}$$

where σ^* and k^* are the Stefan-Boltzmann constant and the mean absorption coefficient, respectively. We assume that the temperature differences within the flow such as that the term T^4 may be expressed as a linear function of temperature. Hence, expanding T^4 in a Taylor series about T_∞ and neglecting higher-order terms we get

$$T^4 \cong 4T_\infty^3 T - 3T_\infty^4, \tag{11}$$

In view to Equations (10) and (11), Equation (9) reduces to

$$u\frac{\partial T}{\partial x} + v\frac{\partial T}{\partial y} = (\alpha + \frac{16\sigma^* T_\infty^3}{3\rho c_P k^*})\frac{\partial^2 T}{\partial y^2} + \frac{v}{c_P}\left(\frac{\partial u}{\partial y}\right)^2. \tag{12}$$

From the above equation it is seen that the effect of radiation is to enhance the thermal diffusivity.

3.1 Prescribed surface temperature (PST case)

In this circumstance, the boundary conditions are

$$T = T_w(= T_\infty + A.\left(\frac{x}{l}\right)^2) \quad at \; y = 0,$$
$$T \to T_\infty \quad as \; y \to \infty, \tag{13}$$

where T_w is the temperature at the wall, $T_\infty(\langle T_w \rangle)$ is the free stream temperature and the constant l is chosen as a characteristic length.

On the other hand, we define the non-dimensional temperature $\theta(\eta)$ as

$$\theta(\eta) = \frac{T - T_\infty}{T_w - T_\infty}. \tag{14}$$

Realize that in order to obtain similarity solutions for temperature $\theta(\eta)$ we consider stretched boundary surface with prescribed power law temperature of second grade only (see Abdelkhalek (2006)).

Using Eqs.(5), (6), (13) and (14) we find from Eq. (12)

$$\theta'' + \frac{3\sigma N_R}{3N_R + 4} f\theta' - \frac{6\sigma N_R}{3N_R + 4} f'\theta = -\frac{3\sigma N_R}{3N_R + 4} E_c f''^2. \tag{15}$$

Here, $\sigma = \frac{\upsilon}{\alpha}$ is the Prandtl number, $E_c = \frac{c^2 l^2}{A c_P}$ is the Eckert number and $N_R = \frac{kk^*}{4\sigma^* T_\infty^3}$ is the radiation parameter.

The boundary conditions (13) become

$$\theta(0) = 1, \quad \theta(\infty) \to 0. \tag{16}$$

The local surface heat flux can be expressed as

$$q_w = -k\left(\frac{\partial T}{\partial y}\right)_w + (q_r)_w = -\frac{Ak(4 + 3N_R)}{3N_R} \cdot \left(\frac{x}{l}\right)^2 \cdot \left(\frac{c}{\upsilon}\right)^{\frac{1}{2}} \cdot \theta'(0). \tag{17}$$

By setting $k_0 = \frac{3N_R}{3N_R + 4}$, Eq. (17) becomes

$$q_w = -k\left(\frac{\partial T}{\partial y}\right)_w + (q_r)_w = -\frac{Ak}{k_0} \cdot \left(\frac{x}{l}\right)^2 \cdot \left(\frac{c}{\upsilon}\right)^{\frac{1}{2}} \cdot \theta'(0). \tag{18}$$

One can see from Eq. (18) that in the limiting case $N_R \to \infty$ (i.e., $k_0 \to 1$) the thermal radiation effects can be neglected.

3.2 Prescribed heat flux (PHF case)

In this case, the power-law heat flux on the wall is considered in the form

at $y = 0$: $q_w = -k\left(\frac{\partial T}{\partial y}\right)_w = D\left(\frac{x}{l}\right)^2$,

as $y \to \infty$: $T \to T_\infty$. $\tag{19}$

where D is a constant whose value depends on the fluid.

On the other hand, we define a non-dimensional temperature $g(\eta)$ as

$$g(\eta) = \frac{T - T_\infty}{\frac{D}{k}\left(\frac{x}{l}\right)^2 \left(\frac{v}{c}\right)^{1/2}}. \tag{20}$$

Using Eqs.(5), (6), (19) and (20), we find from the energy equation, Eq. (12)

$$g'' + \frac{3\sigma N_R}{3N_R + 4} fg' - \frac{6\sigma N_R}{3N_R + 4} f'g = -\frac{3\sigma N_R}{3N_R + 4} E_c' f''^2. \tag{21}$$

where $E_c' = \frac{E_c A k}{D}\left(\frac{c}{v}\right)^{1/2}$ is the scaled Eckert number. It is worth citing that we have obtained the same ODE as in PST case (see Eq. (15)).

The boundary conditions can be obtained from Equations (19) and (20) as

$$g'(0) = -1; \ g(\infty) = 0. \tag{22}$$

and in view of Eq. (20), we get

$$T_w = T_\infty + \frac{D}{k}\left(\frac{x}{l}\right)^2 \left(\frac{v}{c}\right)^{1/2} g(0). \tag{23}$$

Taking into account all above, one can analyze thermal boundary layer results for both PST and PHF cases by using an only governing equation as

$$h'' + \sigma k_0 E f''^2 = \sigma k_0 (2hf' - fh') \tag{24}$$

where $k_0 = \frac{3N_R}{3N_R + 4}$, and $h(0) = 1; h(\infty) \to 0; E = E_c$ for PST case, whereas $h'(0) = -1; h(\infty) \to 0; E = E_c'$ for PHF case. Note that by setting $k_0 = 1$ into Eq. (24), the thermal radiation's effect is then neglected. Realize the one-way coupling, that is, the function f influences the function h, but not vice-versa.

At this stage, it is worth citing that, for each numerical solution, either $h'(0)$(PST case) or $h(0)$(PHF case) are iteratively obtained under the simultaneous assumptions

$$h(\infty) \to 0; \ h'(\infty) \to 0. \tag{25}$$

These boundary conditions at infinity correct unphysical behaviours of the solution because, in this manner, temperature profiles approach the ambient conditions in an asymptotical fashion, Cortell (2008a). It should be mentioned here that two different expressions in PST/PHF cases for the Eckert number in the energy equation

have been obtained. The same Eckert number E_c for both PST and PHF cases was assumed by Aliakbar et al. (2009), and this is not correct. Also, in their PHF energy equation, Eq. (14) in its right hand side, one must replace the factor g''^2 *by* f''^2.

Without a break, we begin now the development of the procedure for completing the solution for $\theta(\eta)$ *and* $g(\eta)$. In general, an analytical solution for the flow problem given by Eqs.(7)-(8) does not exist and, consequently, one has to use numerical techniques. It is clear that the missed velocity gradient at the wall $f''(0)$ in that problem depends on M, K and R. Since the flow problem is uncoupled from the thermal problems, changes in the values of σ, N_R and E_c (E_c') will not affect the fluid velocity. For this reason, both the function f and its derivatives are identical in the complete problem (flow and heat transfer) when M, K and R are given. In view of the above discussions, we have solved numerically, first, the problem {(7)-(8)}, and we have obtained $f''(0)$. Secondly, with these results, we shall solve numerically the complete problem (i.e., momentum and heat transfers) as explained below. This procedure has already been applied to discuss some flow and heat transfer problems, Cortell (1994), (2006a, b), (2008b).

We run now to explain how to obtain a temperature profile in PST case ($\theta-$ *profiles*). Equations (7) and (24) can easily be written as the equivalent first-order system

$$w_1' = w_2$$

$$w_2' = w_3$$

$$w_3' = \frac{2Kw_1w_2w_3 - w_2^2 + w_1w_3 - Mw_2}{Kw_1^2 - 1}$$

$$w_4' = w_5$$

$$w_5' = \sigma k_0(2w_2w_4 - w_1w_5) - \sigma k_0 E_c w_3^2 \tag{26}$$

where the prime indicates differentiation with respect to η, $w_1 = f$, $w_4 = \theta$ and the values of $w_3(0) = f''(0)$ are known either accordingly Table 1 or solving previously the decoupled Eq. (7) along with the boundary conditions given by Eq. (8).

In accordance with conditions (8) and (16) we obtain

$$w_1(0) = R;\ w_2(0) = 1;\ w_4(0) = 1, \tag{27}$$

$$w_2(\infty) = 0;\ w_4(\infty) = 0. \tag{28}$$

Using numerical methods of integration and disregarding temporarily the conditions (28), a family of solutions of {(26)-(27)} can be obtained for arbitrarily chosen values of

$w_5(0) = \left(\frac{d\theta}{d\eta}\right)_{\eta=0}$. Tentatively we assume that a special value of $|\theta'(0)|$ yields a solution for which $\theta(\eta)$, $\theta'(\eta)$ vanishes at a certain $\eta = \eta_\infty$ (see second condition (28)) and satisfies the following conditions

$$w_2(\eta_\infty^\circ) = 0; \; w_4(\eta_\infty) = w_5(\eta_\infty) = 0, \tag{29}$$

where the solution reaches its asymptotic state.

Taking $w_3(0)$ from Table 1, we guess $w_5(0)$ and integrate equations (26) and conditions (27) as an initial value problem by employing a Runge-Kutta algorithm for high-order initial value problems with the additional conditions (29).

$\theta'(0)\langle 0$ implies that heat flows from the surface to the ambient fluid (i. e., $T_w \rangle T_\infty$) and in accordance with Equation (14) a negative θ is not realistic. Consequently, for a physically consistent numerical result, the corresponding θ is everywhere finite and non negative. In PHF case we proceed analogously by setting boundary conditions (22) and guessing $g(0)$ in our shooting procedure.

Figure 3a has been obtained for the case of $R = 0.3$ (suction); $M = 0.5$; $\sigma = 3$; $E_c = 0.1$ and $N_R = 1$ in PST case. As shown in this figure, the elasticity level of the Maxwellian fluid has a strong effect on the temperature profiles. For Maxwell fluids, and for the case of non-zero magnetic field, namely $M = 0.5$, one immediately observes that an increase in the fluid's elasticity appears to increase the temperature profiles at any given point above the sheet. This leads to a lower temperature gradient at the wall with a subsequent drop in the rate of cooling. Thus, it is expected that an increase in the elasticity level of the fluid decreases the total amount of heat transfer from the sheet to the fluid. As expected, a similar trend occurs in PHF case (see Fig. 3b).

On the other hand, from Fig.3a it is found that, irrespective of K, all the curves $\theta'(\eta)$ pass the same point. In other words, for each fixed Prandtl number σ and for a selected set of parameters R, M, E_c and N_R, our procedure is able to encounter two relevant results which are K-independent, that is, $\eta_{K-independent}$ and $\theta'(\eta_{K-independent.})$. Specifically, from Fig. 3a (PST case) we find $\eta_{K-independent} = 2.08$ and $\theta'(\eta_{K-independent}) = -0.146$. The latter is not affected by the elasticity level of the Maxwell fluid. On the other hand, Figs. 3a and 3b reveal that, at selected values of R, M, σ $E_c(E_c')$ and N_R, the dimensionless surface temperature $\theta(\eta)$ of the fluid in PST case is larger than that of the PHF case.

Also, a selected set of numerical solutions for both PST/PHF cases are plotted in Figs. 4-7. We can observe from these figures that the effect of increasing σ is to decrease the temperature distribution, whereas an opposite behaviour can be seen for the Eckert number $E_c(E_c')$. Also, the effect of viscous dissipation becomes more important with the increase of σ.
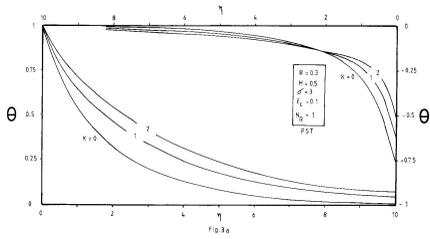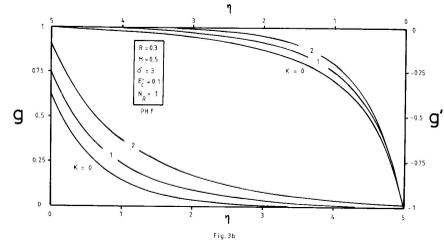
(a)   (b)

Figure 3: a) Temperature and temperature-gradient profiles in PST case for $K = 0$, 2 with suction ($R = 0.3$) and magnetic field ($M = 0.5$) when $\sigma = 3$, $E_c = 0.1$ and $N_R = 1$. b) The same, but in PHF case.

Figures 4a and 4b show the effect of the magnetic field parameter, M, on the temperature profiles above the sheet in both PST/PHF cases in the presence of viscous dissipation, suction and thermal radiation. One can see from these two figures that the magnetic field has a relevant effect on the temperature distributions above the sheet. In fact, for both PST/PHF cases, an increase in the strength of the magnetic field appears to increase the temperature distributions. This means a lower temperature gradient at the wall with a subsequent drop in both the heat flux and the rate of cooling. Further, these commented effects become slightly more significant with the decrease of σ.
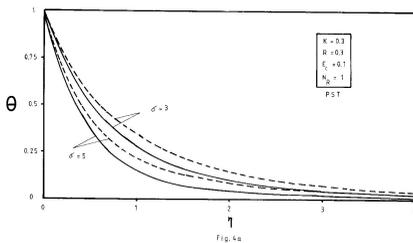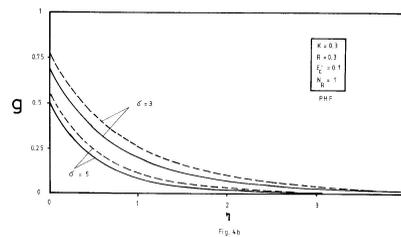
(a)   (b)

Figure 4: a) Plot of temperature distributions in PST case for two values of M and σ when $K = 0.3$, $R = 0.3$, $E_c = 0.1$ and $N_R = 1$. [$M = 1$ (solid line); $M = 3$ (broken line)]. b) The same, but in PHF case.

Suction is applied to chemical processes to remove reactants and, consequently,

we also present in Figs. 5a-b its effects for a Maxwellian fluid in the presence of magnetic field, viscous dissipation and thermal radiation. Our results indicate that a rise in suction parameter R depresses temperature profiles in both PST and PHF cases.
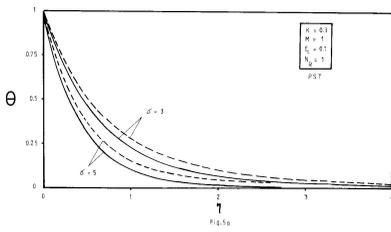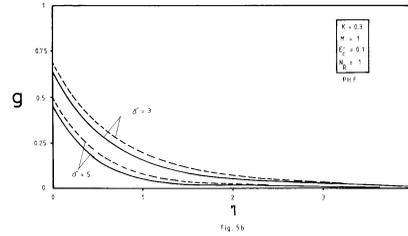
(a)   (b)

Figure 5: a) Plot of temperature distributions in PST case for two values of R and σ when $K = 0.3$, $M = 1$, $E_c = 0.1$ and $N_R = 1$. [$R = 0.6$ (solid line); $R = 0.3$ (broken line)]. b) The same, but in PHF case.

On the other hand, Figs. 6a-b depict the effect of the Eckert number $E_c(E_c')$ for two selected values of σ on temperature profiles. It is evident from these figures that for given values of K, R, M and N_R higher temperatures of fluid elements near the wall are observed at a larger values of $E_c(E_c')$, but this trend is slightly reversed far away from the edge.
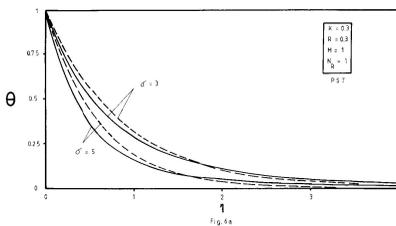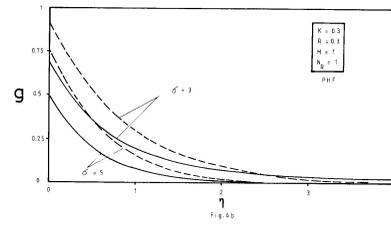
(a)   (b)

Figure 6: a) Plot of temperature distributions in PST case for two values of E_c and σ when $K = 0.3$, $R = 0.3$, $M = 1$ and $N_R = 1$. [$E_c = 0.1$ (solid line); $E_c = 0.5$ (broken line)]. b) The same, but in PHF case.

In addition, from Figs. 7a-b one can see that the effect of radiation becomes more important for a smaller Prandtl number σ by comparing the curves with $\sigma = 3$ and $\sigma = 5$. This implies that sensibility to thermal radiation in Maxwellian flows is enhanced at smaller Prandtl number σ. It is further obvious that the temperature is decreased with an increase in N_R, and as expected, (see for example Abbasi et al. (2011)) the thermal radiation significantly affects temperature distributions.

| (a) | (b) |
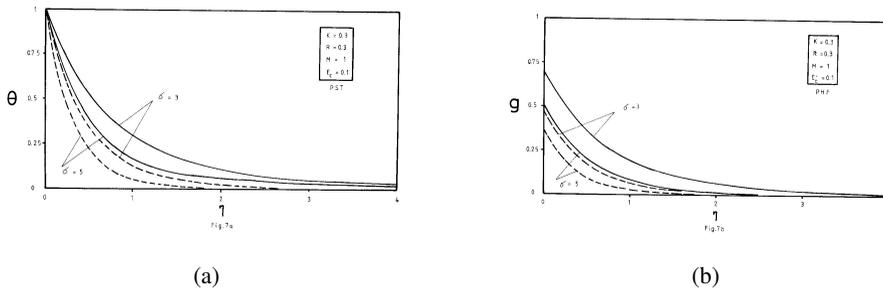
Figure 7: a) Plot of temperature distributions in PST case for two values of N_R and σ when $K = 0.3$, $R = 0.3$, $M = 1$ and $E_c = 0.1$. [$N_R = 1$ (solid line); $N_R = 5$ (broken line)]. b) The same, but in PHF case.

At this stage, it is worth citing that, flow kinematics modifications have already been studied by means of K, M and R flow parameters. Finally, in order to more fully characterize the behaviour of the quantities of relevant physical interest like $\theta'(0)$ *and* $g(0)$ with changes in K, M and R for specified values of σ, $E_c (E_c')$ and N_R, Table 3 is constructed. One can then see from Table 3 that, for both PST/PHF cases, the combined effect of increasing values of K and M is to boost temperature distributions, while the effect of increasing values of R is to depress it.

4   Concluding Remarks

Effects of suction, viscous dissipation and radiation on heat transfer behaviour for an upper-convected Maxwell fluid over a non-isothermal moving flat surface which is linearly stretched (i.e., Crane flow) in the presence of a transverse magnetic field are studied.

The problem under investigation is of the type of one-way coupled problem. This is because due to the fact all properties are considered constant, the velocity boundary value problem (the f-problem) is decoupled from the temperature problems (the θ-g problems), but not vice-versa. Unlike in Sadeghy et al. (2005) occurs, it

Table 3: Kinematic influences on heat transfer characteristics.

R	K	M	σ	$E_c(E_c')$	N_R	$-\theta'(0)$	$g(0)$
0	0.3	1	3	0.1	1	1.338413	0.760088
0.3						1.493146	0.688990
0.6						1.651849	0.632545
0.3	0.3	1	3	0.1	1	1.493146	0.688990
	0.6					1.423968	0.723115
0.3	0.3	0	3	0.1	1	1.613278	0.635143
		0.5				1.548661	0.663334
		1				1.493146	0.688990

admits similarity solutions which are governed by an only ODE (Eq.24), describing fundamental physically significances and we obtain accurate numerical results via the 4th order Runge-Kutta method along with shooting procedure. We found that there was always a marked influence on temperature profiles due to change in the parameters entering the problem. As here it clearly brings out, one can analyze the effects that strength of magnetic field have on the flow (through the parameter M) as well as to directly asses how the suction parameter R affects the non-dimensional velocity and temperature distributions due to its changes. With the help of tables and graphs, a variety of different effects due to change in any other one parameter for fixed values of the remaining parameters is also presented. We saw throughout this original research interesting trends which are in agreement with the researches of the field (see Aliakbar et al. (2009)). From the computational results and for both PST/PHF cases, the following conclusions may be drawn:

1. Effects on non-dimensional velocity:

    (a) An increase in suction (through the parameter R) decreases the velocity field.

    (b) An increase in magnetic field (through the parameter M) decreases the velocity field.

    (c) An increase in the elasticity level of the UCM fluid (through the parameter K) decreases the velocity field.

    One can then conclude that the combined effect of increasing values of R, M and K is to decrease the velocity distribution in the flow region.

2. Effects on temperature distributions:

(a) An increase in suction parameter yields a decrease in the fluid's temperature

(b) An increase in magnetic field increases the temperature field

(c) An increase in the elasticity level of the fluid provides an augment in the fluid's temperature

(d) The increase of the Prandtl number σ leads to the decrease of dimensionless surface temperature

(e) An augment in the Eckert number $E_c(E_c')$ boosts temperature profiles

(f) An increase in radiation parameter N_R depresses temperature distributions.

One can also then conclude that the combined effect of increasing values of R, σ and N_R is to reduce temperature distributions, while the combined effect of increasing values of M, K and $E_c(E_c')$ is to boost temperature distributions.

References

Abbas, Z.; Sajid, M.; Hayat, T. (2006): MHD boundary-layer flow of an upper-convected Maxwell fluid in a porous channel. *Theor. Comput. Fluid Dyn.*, vol 22 no. 4, pp. 229-238.

Abbasi, M. A.; Halouani, K.; Chesneau, X.; Zeghmati, B. (2011): Combined thermal radiation and laminar mixed convection in a square open enclosure with inlet and outlet ports. *Fluid Dynamics & Materials Processing* vol. 7 no. 1, pp. 71-96.

Abdelkhalek M. M. (2006): The skin friction in the MHD mixed convection stagnation point with mass transfer. *Int. Comm. Heat Mass Transfer,* vol. 33, pp. 249-258.

Abo-Eldahab E. M. and Salem A. M. (2004): Hall effects on MHD free convection flow of a non-Newtonian power-law fluid at a stretching surface. *Int. Comm. Heat Mass Transfer,* vol. 31, pp. 343-354.

Aliakbar, V.; Alizadeh-Pahlavan, A.; Sadeghy, K. (2009): The influence of thermal radiation on MHD flow of Maxwellian fluids above stretching sheets. *Comm. Nonlinear Sci. Num. Simul.*, vol. 14 no. 3, pp. 779-794.

Alizadeh-Pahlavan, A., Sadeghy, K. (2009): On the use of homotopy análisis method for solving unsteady MHD flow of Maxwellian fluids above impulsively stretching sheets. *Comm. Non-Linear Sci. Num. Simulat.,* vol. 14 no. 4, pp. 1355-1365.

Amir, A.-P.; Aliakbar, V.; Farzad V.-F.; Sadeghy, K. (2009): MHD flows of UCM fluids above porous stretching sheets using two-auxiliary-parameter homotopy analysis method. *Comm. Nonlinear Sci. Num. Simul.*, vol. 14 no. 2, pp. 473-488.

Bataller, R. C. (2010): Towards a numerical benchmark for MHD flows of Upper-Convected Maxwell (UCM) fluids over a porous stretching sheet. *Fluid Dynamics &Materials Processing*, vol. 6 no. 3, pp. 337-350.

Bhatnagar, R. K.; Gupta, G.; Rajagopal, K. R. (1995): Flow of an Oldroyd-B fluid due to a stretching sheet in the presence of a free stream velocity. *Int. J. Non-Linear Mech.*, vol. 30, pp. 391-405.

Bird, R. B.; Curtiss, C. F.; Armstrong, R. C.; Hassager, O. (1987): *Dynamics of Polymer Liquids, Vol. 2. Kinetic Theory*, Willey, New York, 2nd Ed.

Cortell, R. (1994): Similarity solutions for flow and heat transfer of a viscoelastic fluid over a stretching sheet. *Int. J. Non-Linear Mech.*, vol. 29, pp. 155-161.

Cortell, R. (2005a): A note on magnetohydrodynamic flow of a power-law fluid over a stretching sheet. *Appl. Math. Comput.*, vol. 168, pp. 557-566.

Cortell, R. (2005b): Flow and heat transfer of a fluid through a porous medium over a stretching surface with internal heat generation/absorption and suction/blowing. *Fluid Dyn. Res.*, vol. 37, pp. 231-245.

Cortell, R. (2005c): Numerical solutions of the classical Blasius flat-plate problem. *Appl. Math. Comput.*, vol. 170, pp. 706-710.

Cortell, R. (2006a): A note on flow and heat transfer of a viscoelastic fluid over a stretching sheet. *Int. J. Non-Linear Mech.*, vol. 41, pp. 78-85.

Cortell, R. (2006b): Effects of viscous dissipation and work done by deformation on the MHD flow and heat transfer of a viscoelastic fluid over a stretching sheet. *Phys. Lett. A*, vol. 357, pp. 298-305.

Cortell, R. (2006c): MHD boundary-layer flow and heat transfer of a non-Newtonian power-law fluid past a moving plate with thermal radiation. *Il Nuovo Cimento B,* vol. 121 no. 9, pp. 951-964.

Cortell, R. (2006d): Flow and heat transfer of an electrically conducting fluid of second grade over a stretching sheet subject to suction and to a transverse magnetic field. *Int. J. Heat Mass Transfer,* vol. 49, pp. 1851-1856.

Cortell, R. (2007a): MHD flow and mass transfer of an electrically conducting

fluid of second grade in a porous medium over a stretching sheet with chemically reactive species. *Chem. Eng. Proc.*, vol. 46, pp. 721-728.

Cortell, R. (2007b): Toward an understanding of the motion and mass transfer with chemically reactive species for two classes of viscoelastic fluid over a porous stretching sheet. *Chem. Eng. Proc.: Proc. Intens.*, vol. 46, pp. 982-989.

Cortell, R. (2007c): Viscoelastic fluid flow and heat transfer over a stretching sheet under the effects of a non-uniform heat source, viscous dissipation and thermal radiation. *Int. J. Heat Mass Transfer,* vol. 50, pp. 3152-3162.

Cortell, R. (2007d): Effects of heat source/sink, radiation and work done by deformation on flow and heat transfer of a viscoelastic fluid over a stretching sheet. *Comput. Math. Appl.*, vol. 53, pp. 305-316.

Cortell, R. (2008a): A numerical tackling on Sakiadis flow with thermal radiation. *Chin. Phys. Lett.*, vol. 25, pp.1340-1342.

Cortell, R. (2008b): Similarity solutions for boundary layer flow and heat transfer of a FENE-P fluid with thermal radiation. *Phys. Lett. A,* vol. 372 no.14, pp. 2431-2439.

Cortell, R. (2008c): Analysing flow and heat transfer of a viscoelastic fluid over a semi-infinite horizontal moving flat plate. *Int. J. Non-Linear Mech.*, vol. 43, pp. 772-778.

Cortell, R. (2010): On a certain boundary value problem arising in shrinking sheet flows. *Appl. Math. Comput.*, vol. 217 no. 8, pp. 4086-4093.

Chen, C.-H. (2009):*Magneto-hydrodynamic mixed convection of a power-law fluid past a stretching surface in the presence of thermal radiation. Int. J. Non-Linear Mech.*, vol. 44 no. 6, pp 596-603.

Crane, L. J. (1970): Flow past a stretching plate. *ZAMP*, vol. 21, pp 645-647.

Dandapat, B. S.; Gupta, A. S. (1989): Flow and heat transfer in a viscoelastic fluid over a stretching sheet. *Int. J. Non-Linear Mech.*, vol. 24, pp. 215-219.

Hayat, T.; Sajid, M. (2007): Homotopy analysis of MHD boundary layer flow of an upper-convected Maxwell fluid. *Int. J. Eng. Sci.*, vol. 45, pp. 393-401.

Hayat, T., Abbas, Z. (2008): Channel flow of a Maxwell fluid with chemical reaction. *ZAMP*, vol. 59, pp 124-144.

Hayat, T.; Abbas, Z.; Sajid, M. (2006): Series solution for the upper-convected Maxwell fluid over a porous stretching plate. *Phys. Lett. A*, vol. 358, pp. 396-403.

Liu C.-S., Chang J-.R. (2008): The Lie-group shooting method for multiple-solutions of Falkner-Skan equation under suction-injection conditions. *Int. J. Non-Linear Mech.*, vol. 43, pp. 844-851.

Nazar R., Amin N. and Pop I. (2004): Unsteady boundary layer flow due to a stretching surface in a rotating fluid. Mech. Res. Comm., vol. 31, pp. 121-128.

Rajagopal, K. R., Na T. Y. and Gupta A. S. (1984): Flow of a viscoelastic fluid over a stretching sheet. *Rheol. Acta*, vol. 23, pp. 213-215.

Sadeghy K., Hajibeygi H. and Taghavi S-H (2006): Stagnation-point flow of upper-convected Maxwell fluids. *Int. J. Non-Linear Mech.*, vol. 41, pp. 1242-1247.

Sadeghy, K., Najafi, A.-H. and Saffaripour, M. (2005): Sakiadis flow of an upper-convected Maxwell fluid. *Int. J. Non-Linear Mech.*, vol. 40, pp 1220-1228.

Sakiadis, B. C. (1961): Boundary-layer behaviour on continuous solid surfaces. The boundary-layer on a continuous flat plate. *AIChE J.*. vol. 7, pp. 221-225.

Singh A. K. (2008): Heat source and radiation on magneto-convection flow of a viscoelastic fluid past a stretching sheet: Analysis with Kummer's functions. *Int. Comm. Heat Mass Transfer*, vol. 35, pp. 637-642.

Subhas Abel, M., Datti, P. S., Mahesha, N. (2009): Flow and heat transfer in a power-law fluid over a stretching sheet with variable thermal conductivity and non-uniform heat source. *Int. J. Heat Mass Transfer*, vol. 52 no.11-12, pp. 2902-2913.

Winter H. H. (1977): Viscous dissipation in shear flows of molten polymers. *Adv. Heat Trans.*, vol. 13, 280.